

# Bends and Momentum Dispersion during Final Compression in Heavy Ion Fusion Drivers

Edward P. Lee<sup>1</sup> and John J. Barnard<sup>1,2</sup>,

1. LBNL, Berkeley, CA, 94720 USA; 2. LLNL, Livermore, CA 94550, USA

## Abstract

Between the accelerator and fusion chamber the heavy ion beams are subject to a dramatic but vital series of manipulations, some of which are carried out simultaneously and involve large space charge forces. The beams' quality must be maintained at a level sufficient for the fusion application; this general requirement significantly impacts beam line design, especially in the considerations of momentum dispersion. Immediately prior to final focus onto a fusion target, heavy ion driver beams are compressed in length by typically an order of magnitude. This process is simultaneous with bending through large angles to achieve the required target illumination configuration. The large increase in beam current is accommodated by a combination of decreased lattice period, increased beam radius, and increased strength of the beamline quadrupoles. However, the large head-to-tail momentum tilt (up to 5%) needed to compress the pulse results in a very significant dispersion of the pulse centroid from the design axis. General design features are discussed. A principal design goal is to minimize the magnitude of the dispersion while maintaining approximate first order achromaticity through the complete compression/bend system. Configurations of bends and quadrupoles, which achieve this goal while simultaneously maintaining a locally matched beam-envelope, are analyzed.

## 1. INTRODUCTION

Conceptual heavy ion driver systems for inertial fusion energy generally require multiple high power ion pulses of very short duration on the fusion target to achieve an efficient implosion of the fusion capsule. Typically, this might be made up of 84 separate beams of 2.5 GeV Cs<sup>+</sup>, each with 2.0 kA and 10 ns duration. Such short pulses cannot be accelerated effectively using induction linac technology so drift compression by about an order of magnitude between the linac and the final focus system is employed. Several novel features of beam dynamics arise simultaneously in this compression zone. The high currents are confined by quadrupoles in a FODO configuration, with bends located in the drift sections or in combined function to achieve the desired system configuration. Bends are included in a driver between the accelerator and target for several reasons. These include achieving symmetric illumination, separating beams for final focus, removing line-of-sight neutrons, and to layout delay

lines if needed. In this paper we address some dynamical and design features associated with the bend systems involved in transporting the beams from the accelerator to the vicinity of the fusion chamber. This section typically may be 400m in length and include about 100 bend magnets per beam channel. Bending is primarily in the horizontal plane and typically includes both positive and negative arcs, which add up to a net 90° turn (see Figure 1). Pulse compression in time proceeds throughout the driver system, primarily due to acceleration, while pulse length as measured in meters typically only decreases by a factor of about four in the linac. These features of the driver system are apparent in Figure 2. The beam is typically 5.0m in length at the end of the linac and must be further compressed to about .5m before final focus.

To compress a beam pulse, a head-to-tail velocity tilt of several percent is applied during the final stages of acceleration in the linac (DE HOON, M.J.L. *et al.* 2002). The initial magnitude of the tilt  $\tau = (v_T - v_H)/v_0$  is approximately equal to the ratio of the initial pulse length (in m) to the drift distance. This ratio is typically in the range  $.02 \leq \tau \leq .1$ . The larger figure is associated with high perveance beams (see eqn. (1)) that are associated with short drift compression lengths and bend arcs with small radii of curvature. In these circumstances we expect dispersion of the beams' centroids to be a very significant feature of the dynamics (LEE, E.P. *et al.* 1987). Current rises steadily during compression and this requires that either the beam radius increase or the lattice period length to decrease simultaneously. Quadrupole field strength at the beam edge also increases along the system. Roughly, the dimensionless generalized perveance  $Q$  is related to the lattice period length ( $P$ ) and the mean beam edge radius ( $\bar{a}$ ) by the space charge limit:

$$\frac{2qI}{4\pi\epsilon_0(\beta\gamma)^3 mc^3} \equiv Q \approx 1.4 \frac{\bar{a}^2}{P^2}, \quad (1)$$

where we have taken the undepressed lattice tune to be  $\sigma_0 = 72^\circ$  per period. Here  $I$  is the beam current,  $q$  is the ion charge,  $m$  is the ion mass,  $\beta\gamma mc$  is the ion momentum, and  $\epsilon_0$  is the permittivity of free space. If  $P$  is held at a low constant value to limit dispersion then  $\bar{a}$  is seen to increase as  $I^{1/2}$ .

Any segment of a beam pulse has momentum deviation  $\Delta \leq \tau/2$ . Bends kick the segment away from the design orbit by incremental angle  $\Delta \ell_B / \rho$ , where  $\ell_B$  is the bend length and  $\rho$  is the radius of curvature of the design orbit within the bend.

Quadrupoles, on the average, push the beam segment back towards the design orbit. A rough measure of the sideways displacement of the beam centroid ( $x$ ) is obtained from the matched smooth limit formula where

$$0 = x'' = -\left(\frac{\sigma_0}{P}\right)^2 x + \frac{\Delta}{\langle \rho \rangle}, \quad (2) \quad \langle \rho \rangle$$

the local curvature of the design orbit and  $\Delta$  is local fractional momentum deviation. For example:  $\rho = 50$  m,  $\Delta = 0.02$ ,  $\sigma_0 = 72^\circ$ , and  $P = 3.0$  m yields the matched value  $x = 2.3$  mm. A critical question is whether the dispersion  $x(z)$  of a beam segment remains in a matched state with only small amplitude oscillations while the lattice and beam parameters change. Furthermore, it is desirable that the entire pulse enters the final focus system essentially on axis, i.e. the system is globally achromatic. There is no simple principle of design that will guarantee these features for a single segment of a pulse, let alone for the entire pulse. However, we find ample evidence from numerical analysis that an “adiabatic” variation of lattice features will suffice. That is, if  $\langle \rho \rangle$ ,  $I$ , and  $P$  vary slowly on the scale of a betatron wavelength, the dispersion, as well as the beam envelope may remain in a nearly matched condition. Since there does not appear to be a developed mathematical basis for this strategy, it must be verified by numerical examples.

Equations (1) and (2) suggest several design principles. First, there is a strong economic motive to make  $P$  short when  $Q$  is large since this makes the beam radius small. However, high quadrupole field strength generally puts a lower limit on  $P$  in this case. We also see that the ratio  $x/a$  is proportional to  $P/\sqrt{Q}$ ; this suggests the desirability of small  $P$  early in compression. Small, constant  $P$  throughout the entire bend/compression system is therefore a reasonable design strategy, which we adopt, in the numerical examples in this work.

There has been very little previous study of dispersion in HIF driver scale final compression systems and little is known about the resulting aberrations and emittance growth. The features of large perveance and large, variable tilt make existing single particle formalism (WENG, W.T *et al.* 1989) and codes largely inapplicable. In order to make a start on this topic we adopt a “point model” for a beam segment that includes the main forces acting on it in an approximate fashion (Section 2). In this study of the beam centroid dispersion and envelope during drift compression in bends, model equations are integrated using a simple Mathematica® code. The model assumptions are: 1. KV envelope equations for beam radii in the  $x$  (i bend plane) and  $y$  (vertical) directions. 2. A centroid equation, which includes: image forces, off-momentum slices from velocity tilt, and non-linearity in  $\Delta$ . 3. A longitudinal envelope equation based on a constant g-factor model for calculating the longitudinal space charge force. 4. Discrete bend and

quadrupole elements. The lattice period, focusing strength and perveance are allowed to vary with  $z$ . The goal is to try to minimize dispersion throughout the bend system and particularly the final centroid values of  $x$  and  $x'$  at exit of the bend system. For this study, the parameters were those typical of a Heavy Ion Fusion (HIF) “driver”, see Table 1.

Table 1. Parameters used in this study. Parameters are typical of what is expected for an HIF “driver”.

Parameter	Value
Charge state (q/e)	1
Ion Mass (amu)	132.9
Ion Energy (GeV)	2.43
Initial Current per beam at accel. exit (A)	103.4
Final Current per beam (A)	2254
Compression Factor	21.8
Final Perveance $Q$	0.000181
Velocity tilt (Dv/v)	-0.031
Total drift length (m)	502.3
Beam radius evolution	$a \sim \sqrt{Q/Q_0}$
Lattice period evolution	$L \sim \text{constan}$

## 2. MODEL EQUATIONS AND EXAMPLE PARAMETERS

Four simultaneous equations are solved:

$$\frac{d^2 \ell}{dz^2} = \frac{12gqC}{4\pi\epsilon_0\gamma^5 m v_0^2} \frac{1}{\ell^2} - k_L \ell, \quad (3)$$

$$\frac{d^2 x}{dz^2} = \frac{1}{\rho_0} \left(1 - \frac{p_0}{p}\right) - \frac{qG}{p} x + \frac{Q}{R} \left[ \frac{x}{R} + \left( \frac{x^2 + (a^2 - b^2)/4}{R^3} \right) x \right], \quad (4)$$

$$\frac{d^2 a}{dz^2} = \frac{\epsilon_N^2}{\beta^2 \gamma^2 a^3} - \frac{qG}{p} a + 2Q \left[ \frac{1}{a+b} + \left( \frac{x^2 + (a^2 - b^2)/4}{2R^3} \right) \frac{a}{R} \right], \quad (5)$$

$$\frac{d^2 b}{dz^2} = \frac{\epsilon_N^2}{\beta^2 \gamma^2 b^3} + \frac{qG}{p} b + 2Q \left[ \frac{1}{a+b} - \left( \frac{x^2 + (a^2 - b^2)/4}{2R^3} \right) \frac{a}{R} \right] - \frac{b}{\rho_0^2}. \quad (6)$$

Here  $\ell$  is the bunch length,  $x$  is the centroid position,  $a$ ,  $b$  are the envelopes in the  $x, y$  -directions,  $q$  is the ion charge,  $m$  is the ion mass,  $v_0$ ,  $p_0, \gamma$  are the central ion velocity, momentum, and Lorentz factor;  $p$  is the particular ion momentum of the segment;  $\rho_0$  is the instantaneous radius of curvature of the design orbit,  $G$  is the quadrupole gradient;  $R$  is the pipe radius;  $k_L$  is the longitudinal focusing coefficient ( $k_L$  vanishes in the drift section),  $\epsilon_N$  is the normalized emittance,  $C$  is the total charge in each beam, and  $\epsilon_0$  is the permittivity of free space. We assume that the pulse evolves self-similarly with a parabolic line charge density  $\lambda$  satisfying  $\lambda = 3C(1 - 4\zeta^2/\ell^2)/(2\ell)$  for  $|\zeta/(\ell/2)| \leq 1$  and slice momentum satisfies  $p/p_0 = 1 + \ell'\zeta/\ell$ , where  $\zeta$  is

the slice position relative to the bunch center, with  $\zeta/\ell$  constant for each beam segment.

### 3. BEND STRATEGIES

We consider three design strategies for placing bends in a drift compression lattice: 1. Abrupt bends, in which all bends are full strength. This is the simplest configuration from which to compare improved designs. 2. Matched bends: Here we choose bends of half-strength over a distance equal to one-half of the undepressed betatron period. The centroid will enter the full strength section at the peak of the amplitude of a half-strength bend centroid betatron orbit, with  $x' \approx 0$  (in the smooth focusing approximation). This will be close to the matched condition for a full strength bend, and hence subsequent bends are at full strength. 3. Adiabatic bend: In this design strategy, a gradual ramp-up of bend strength over several betatron periods is carried out, keeping centroid and envelope oscillations “matched” at low amplitude. Figure 2 illustrates three generic half-lattice periods for all three design strategies.

### 4. COMPARISON OF THE BEND STRATEGIES



Figure 1. Induction linac system

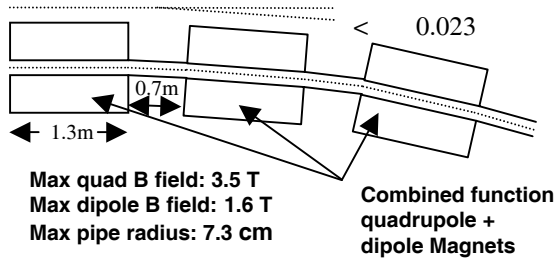


Figure 2. Schematic layout of three half-lattice periods of the example pulse compression line. Note that the beam and pipe radius as well as the bending strength vary along the beamlines. We have adopted combined quadrupole and bend elements in this study.

Figures 3a, 3b, and 3c illustrate the layout of instantaneous radius of curvature of the bend centroid using bend strategies 1-3 respectively.

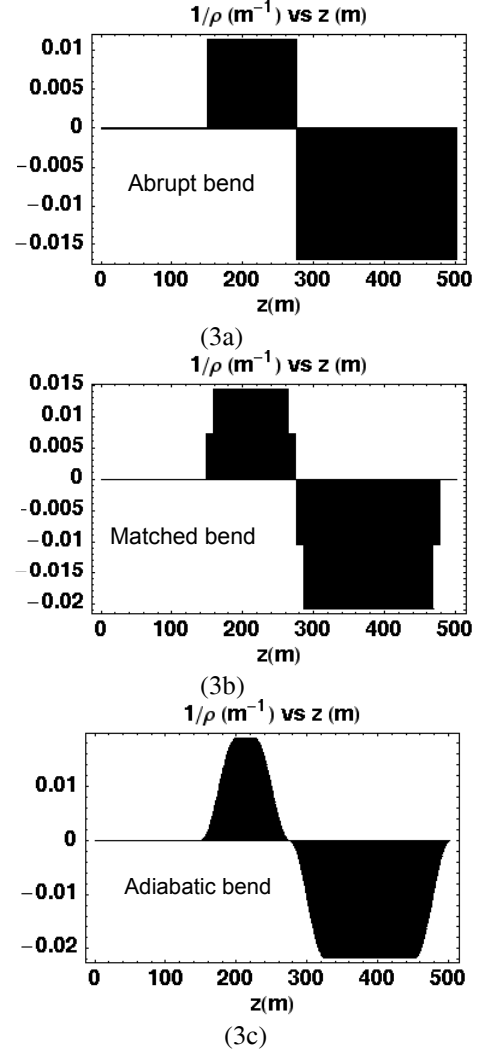


Figure 3. Inverse instantaneous radius of curvature ( $\text{m}^{-1}$ ) as a function axial distance (m) for (a) an abrupt bend, (b) a matched bend, and (c) an adiabatic bend, using driver parameters of table 1. Peak strength is shown, with bend occupancy of 0.65.

The bunch length  $\ell$  is undergoing compression in all three scenarios and is found by integration of equation (3). Figure 3 illustrates the evolution of  $\ell$  with  $z$ .

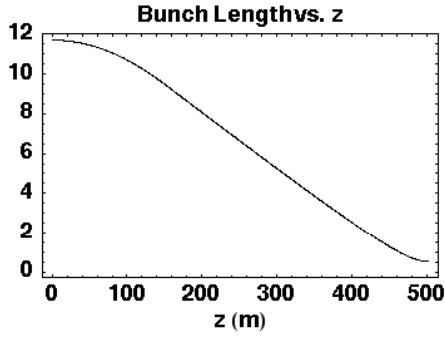
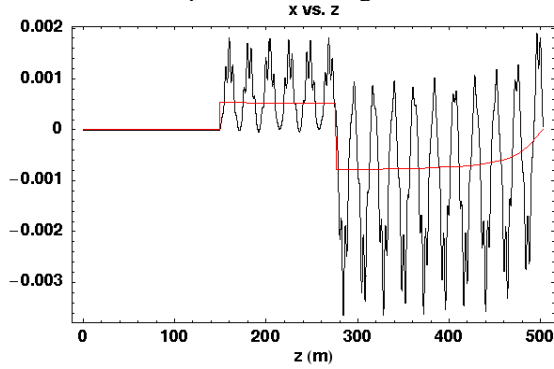
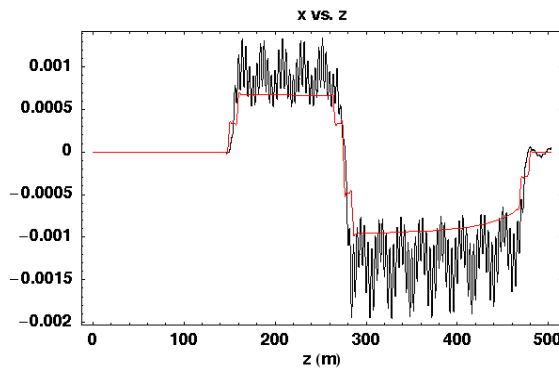


Figure 4. Bunch length  $\ell$  vs.  $z$  for all 3 bend strategies.

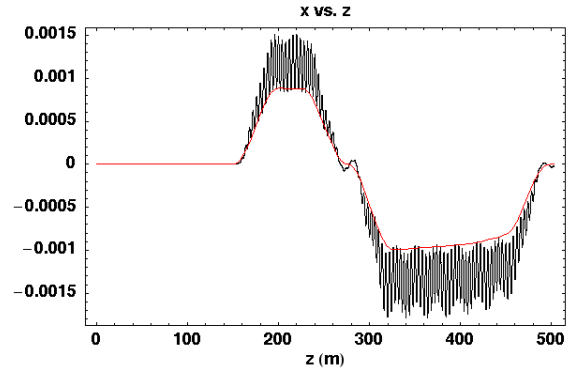
The evolution of the centroid for an off-momentum segment of the beam varies according to which bend scenario is selected. Since bunch compression intrinsically requires the velocity of the beam to systematically vary from tail to head, systematic velocity dispersion is an essential feature of bunch compression; it is assumed that the thermal spread of velocities is insignificant. From Figure 5, it is apparent that the abrupt turn-on of the bend has greatest dispersion and largest  $x'$  upon exit from the bend, whereas the “matched” and “adiabatic” designs have smaller excursions and terminate the bend with little residual centroid displacement or angle.



(5a)



(5b)



(5c)

Figure 5. Evolution of centroid for the beam slice half-way between center and head, in bend design scenarios (a) abrupt, (b) matched, and (c) adiabatic. The solid (non-oscillating) line in each figure represents the instantaneous smooth limit result given by eqn. (2).

## 5. SUMMARY AND CONCLUSIONS

In this paper we have shown the effect of three different bending scenarios on the beam centroid for different longitudinal slices of the beam, (and hence different longitudinal velocities).

An abrupt turn-on of the bend induces a centroid mismatch for off-momentum slices, and does not return the slice to the center of the beamline upon exit of the bend. This would increase the requirement on pipe radius throughout the drift compression section and would lead to an enlargement of the spot on target if not corrected using time dependent steering.

Matched designs in which the bend ramps at about half-strength for half of a betatron period reduce both maximum pipe radius and final centroid displacement, as do adiabatic designs in which the bend strength ramps up and down over several betatron periods. Adiabatic designs appear more robust however, allowing greater flexibility in choice of tune and beam parameters, with minimal penalty in bend length or bend strength.

The authors would like to acknowledge useful conversations with M. de Hoon, S. S. Yu and H. Qin regarding drift compression.

## REFERENCES:

DE HOON, M.J.L. *et al.* Submitted to  
*Physics of Plasmas*, 2002, LBNL-49646.

LEE, E.P. *et al.* 1987 *IEEE Catalog*, No.  
**87CH2387-9**, p. 1126.

WENG, W.T *et al.* 1989 *AIP Conference*  
*Proceedings* **249**, Vol. **1**.

Work performed under the auspices of the U.S. Department of  
Energy under University of California contract W-7405-ENG-48 at  
LLNL, and University of California contract DE-AC03-76SF00098  
at LBNL.